A R C H I V E S O F M E T A L L U R G Y A N D M A T E R I A L S
Volume 58 2013 Issue 2
DOI: 10.2478/amm-2013-0021

K. PRZYBYLSKI*, J. PRAŻUCH*, T. BRYLEWSKI*, E. DURDA*

HIGH TEMPERATURE OXIDATION BEHAVIOUR OF TiAl8Nb ALLOY

BADANIA WYSOKOTEMPERATUROWEGO UTLENIANIA STOPU TiAl8Nb

The goal of this work is to determine the effect of niobium on the kinetics and mechanism of Ti-Al oxidation in air. In order to compare the oxidation kinetics of Ti-Al and Ti-Al with the addition of niobium, isothermal oxidation was performed on Ti-48Al and Ti-46Al-8Nb (in at.%) alloys at 1073 K in synthetic air. Cyclic oxidation of Ti-46Al and Ti-46Al-8Nb alloys was carried out in laboratory air for 42 cycles (1 cycle, 24 hrs). The morphology, as well as chemical and phase composition of the oxidation products were investigated using X-ray Diffraction (XRD) and Scanning Electron Microscopy combined with Energy Dispersive Spectroscopy (SEM-EDS). From these investigations it can be concluded that niobium addition increases the corrosion resistance of TiAl and, furthermore, improves the adherence between the metallic substrate and the oxide scale. The oxidation mechanism of Ti-46Al-8Nb was studied via secondary neutral mass spectroscopy (SNMS) after two-stage isothermal oxidation (24 hrs in $^{16}O_2$ followed by 24 hrs in $^{18}O_2$) at 1073 K. From this analysis it can be assumed that the oxidation mechanism of Ti-46Al-8Nb alloy consists of simultaneous outward titanium and aluminum diffusion and inward oxygen transport.

Keywords: intermetallics, titanium aluminide, niobium, oxidation

Celem pracy jest określenie wpływu dodatku niobu na kinetykę i mechanizm utleniania stopu TiAl w powietrzu. Dla porównania kinetyk utleniania stopu Ti-Al oraz stopu z dodatkiem niobu zostały przeprowadzone badania izotermicznego utleniania stopów o składach Ti-48Al i Ti-46Al-8Nb (w at.%) w powietrzu syntetycznym w 1073 K. Stopy Ti-48Al i Ti-46Al-8Nb poddano cyklicznemu utlenianiu w powietrzu laboratoryjnym w 1073 K obejmującym 42 cykle 24-godzinne. Morfologię oraz skład fazowy i chemiczny produktów utleniania badanych próbek przeprowadzono metodą dyfrakcji promieniowania rentgenowskiego (XRD) oraz skaningowej mikroskopii elektronowej (SEM) w połączeniu z metodą dyspersji energii promieniowania rentgenowskiego (EDS). Na podstawie tych badań stwierdzono, że dodatek niobu w stopie TiAl podwyższa jego odporność korozyjną a ponadto polepsza przyczepność zgorzeliny do rdzenia metalicznego. Mechanizm utleniania stopu Ti-46Al-8Nb badano metodą spektrometrii masowej rozpylonych cząstek neutralnych (SNMS) po dwuetapowym izotermicznym utlenianiu (pierwszy etap w $^{16}O_2$ przez 24 godz., kolejny w $^{18}O_2$ przez 24 godz.) w 1073 K. Na podstawie tej analizy postuluje się, że mechanizm utleniania stopu Ti-46Al-8Nb odbywa się w wyniku równoczesnej odrdzeniowej dyfuzji tytanu i glinu oraz dordzeniowego transportu tlenu.

1. Introduction

Titanium aluminide (TiAl) intermetallic compounds based on the γ phase belong to a prospective group of corrosion-resistant and heat-resistant materials with applications in aerospace, automobile and gas turbine industries due to their low density, high melting temperature, high specific stiffness and good creep resistant properties [1-3]. Unfortunately, γ-TiAl-based alloys can only be used at temperatures below 1073 K due to their poor oxidation resistance [1-7]. Recent research has proven that additions of niobium (Nb) introduced to γ-TiAl-based alloy can improve its oxidation resistance and also affect its structural and mechanical properties [2,7-9]. The beneficial effect of Nb is suggested by "doping mechanism" of the titania lattice by Nb ions or by mechanisms based on bulk properties [5-10]. Oxidation on the intermetallic phase matrix of the Ti-Al system is a complex process, the course of which is dependent on several factors, such as: temperature, composition of the oxidizing air, partial pressure of oxygen, presence of water vapour, alloy surface treatment, composition and microstructure of the alloy and other impurities in the atmosphere. Therefore, different Ti-Al oxidation results can be found in literature [6,7,11-13]. The goal of this research is to determine the influence of niobium (Nb) addition on the heat-resisting properties of the alloy in air, as well as on the high temperature oxidation kinetics in isothermal and cyclic conditions and the mechanism of TiAl high temperature oxidation.

* AGH UNIVERSITY OF SCIENCE AND TECHNOLOGY, 30-059 KRAKÓW, POLAND

2. Experimental procedure

Three alloys with chemical compositions Ti-48Al, Ti-46Al and Ti-46Al-8Nb were investigated in this study. All concentrations in this work are given in at.%. The afore-mentioned samples were synthesized via induction melting in a crucible furnace containing argon atmosphere and centrifugal casting into graphite moulds. The ingots were produced by hot isostatic pressing (HIP) and then were thermally treated with hardening and ageing in order to obtain the desired microstructure. Specimens, 10×10×0.5 mm in size for isothermal oxidation investigations and 20×10×1 mm for cyclic oxidation studies, were cut from the ingots, manually ground using SiC abrasive paper (1000 to 1200 grade) and polished with slurry containing 0.3μm Al_2O_3 powder. Finally, the samples were ultrasonically cleaned in ethanol, dried at room temperature and weighed.

Isothermal oxidation investigations of Ti-48Al and Ti-46Al-8Nb were carried out at 1073 K for up to 170 hrs in synthetic air. A continuous thermogravimetric apparatus with a MK2 microbalance head (C I Electronics, UK) with 10^{-6} g sensitivity was used to measure mass change per unit area of the alloys during the isothermal oxidation process as a function of time.

Cyclic oxidation studies of Ti-46Al and Ti-46Al-8Nb alloys were performed at 1073 K in laboratory air atmosphere. These investigations consisted of 42 cycles (1 cycle, 24 hrs).

The morphology and chemical composition of the products formed on the samples after isothermal and cyclic oxidation were determined using scanning electron microscopy (SEM) combined with energy dispersive spectroscopy (EDS). The phase composition of the previously mentioned products was analyzed via X-ray diffraction (XRD).

3. Results and discussion

3.1. Isothermal oxidation

The results of the isothermal oxidation kinetics of Ti-48Al and Ti-46Al-8Nb alloys at 1073 K after exposure to synthetic air are presented in Fig. 1 according to the parabolic rate relationship (Eq. (1)):

$$(\Delta m/A)^2 = k_p \cdot t + C \tag{1}$$

where $\Delta m/A$ is the weight gain per unit area (g/cm^2), t is time (s), k_p is the parabolic oxidation rate constant (g^2 cm^{-4} s^{-1}), and C is an integration constant defining the onset of parabolic kinetics. This suggests that diffusion processes might determine the rate of the oxide scale growth. It has been found that the oxidation rate of the Ti-46Al-8Nb alloy is half an order lower than that of Ti-48Al at 1073 K.

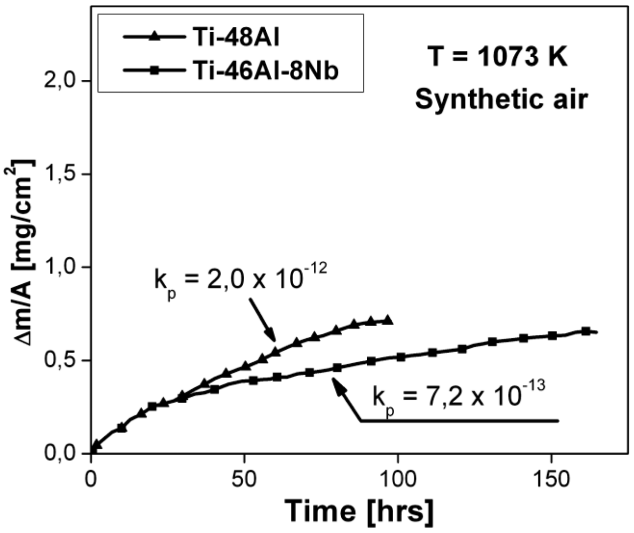

Fig. 1. Isothermal oxidation kinetics of Ti-48Al and Ti-46Al-8Nb at 1073 K in synthetic air (Kp unit: g^{2}cm^{-4}s^{-1})

X-ray Diffraction (XRD) patterns of Ti-48Al and Ti-46Al-8Nb after isothermal oxidation at 1073 K in synthetic air are illustrated in Fig. 2a and Fig. 2b, respectively. Rutile is the dominant phase in the oxide scale formed on Ti-48Al. The presence of corundum and Ti-Al phases from the substrate were also detected. On the other hand, larger amounts of corundum were observed in the oxide scale formed on Ti-46Al-8Nb. Additionally, titanium nitride (TiN), Ti_3O_5 and Ti-Al from the metallic substrate were found. Small amounts of NbO are also visible in the XRD pattern.

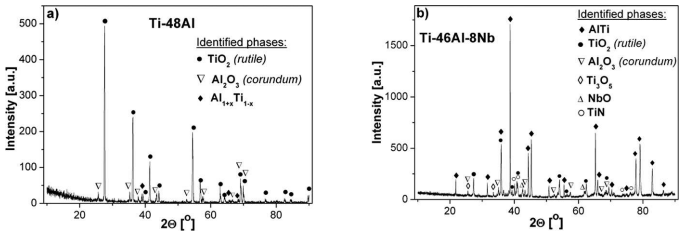

Fig. 2. X-ray Diffraction (XRD) analysis obtained on the surface of a) Ti-48Al and b) Ti-46-Al-8Nb after isothermal oxidation at 1073 K in synthetic air

SEM microstructures of Ti-48Al after isothermal oxidation at 1073 K for 100 hrs and Ti-46Al-8Nb after isothermal oxidation at 1073 K for 170 hrs are shown in Fig. 3a and Fig. 3b, respectively. From these microphotographs it was determined that, for both cases, the scale is well adherent to the metallic substrate and exhibits a multilayer structure. The oxide scale formed on Ti48Al alloy was around 5μm thick and consisted of two layers. The outer layer is around 1.5μm thick and built with TiO_2 plates. The inner layer that adheres to the substrate consists mostly of small TiO_2 grains with some amounts of Al_2O_3. On the other hand, the scale formed on Ti-46Al-8Nb consisted of three layers: a thin surface layer in which Al_2O_3 with a few isolated TiO_2 crystal plates were found; an intermediate layer built from oxides (TiO_2 and Al_2O_3) and an inner layer at the alloy/scale interface, where particles rich in Nb were detected.

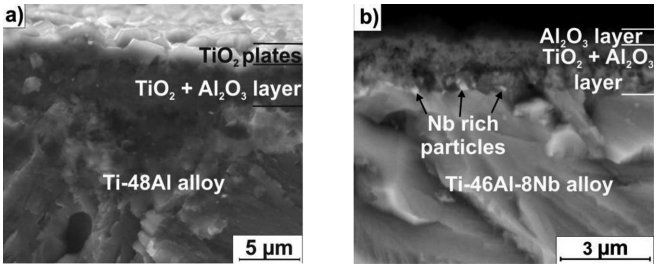

Fig. 3. SEM microphotograph of the fracture cross-section of the oxide scale formed on a) Ti-48Al and b) Ti-46Al-8Nb after isothermal oxidation at 1073 K in synthetic air

In order to determine the oxidation mechanism of the Ti-46Al-8Nb alloy, two-stage isothermal oxidation at 1073 K was carried out for 24 hrs in $^{16}O_2$ followed by 24 hrs in $^{18}O_2$ [14]. The results of this secondary neutral mass spectrometry (SNMS) analysis are presented in Fig. 4. In this figure, the concentration of Ti increases continuously towards the scale/metal interface and the Al and ^{18}O distributions show a maximum at the scale/gas interface which indicates the contribution of the outward cation diffusion in the scale growth and formation of Al_2O_3. However, the location of the ^{18}O second maximum in the portion of the oxide scale enriched in Ti suggests that TiO_2 grows via inward diffusion of oxygen in the inner part of the scale.

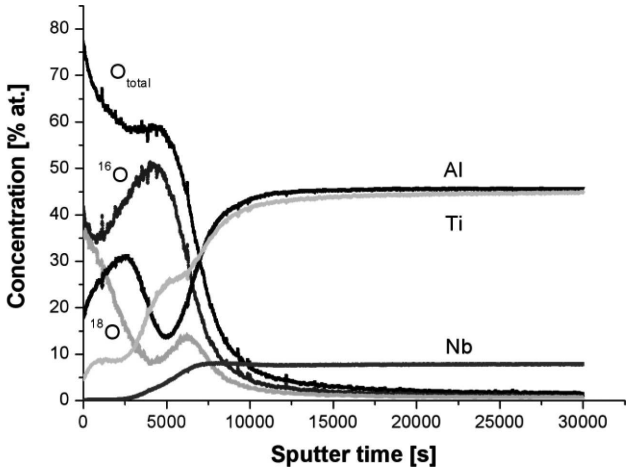

Fig. 4. Quantified SNMS profile of a Ti-46Al-8Nb alloy after two stage oxidation at 1073 K for 24 hrs in $^{16}O_2$ followed by 24 hrs in $^{18}O_2$ [14]

3.2. Cyclic oxidation

The mass changes of the alloy during cyclic oxidation tests give important information on the heat resistance of the studied samples, i.e. the adherence of the scales formed on the samples and their rehealing on exposed metal surfaces. Such investigations of Ti-46Al (Fig. 5a) and Ti-46Al-8Nb (Fig. 5b) alloys were carried out at 1073 K in laboratory air for 42 cycles (1 cycle, 24 hrs). On the basis of this research the net mass change (N) of the samples was determined by Eq. (2):

$$N = \frac{m_{ni} - m_{n0}}{A} \tag{2}$$

Furthermore, the total mass change of a given sample, scale and/or coating collected in a crucible (gross mass change – G) was determined as Eq. (3):

$$G = \frac{m_{gi} - m_{g0}}{A} \tag{3}$$

The mass change of the scale and/or coating collected in the crucible (spall mass change – S) was calculated from Eq. (4):

$$S = G - N \tag{4}$$

where: m_{ni} – mass of the sample after heating-cooling cycle nr i [g], m_{n0} – mass of the sample before the heating-cooling cycle [g], m_{gi} – total mass of the sample and crucible after heating-cooling cycle i [g], m_{g0} - total mass of the sample and crucible before the heating-cooling cycle [g], A – surface area of the sample [cm^2].

In the case of Fig. 5a, systematic linear mass growth of the scale accumulating in the crucible was observed, starting at the first stage of the process. From this, it can be concluded that the adherence of the scale to the metallic substrate is poor. As the scale detaches itself from the substrate, the corrosion process accelerates. However, in Fig. 5b, the cyclic oxidation of Ti-46Al-8Nb alloy approximately follows the parabolic rate law. This means that diffusion of the reactants in the scale is the rate limiting step of the oxidation process. Throughout the entire thermal treatment mass growth of the scale is practically nonexistent, which means that the scale adheres very well to the metallic substrate, creating a compact and smooth layer on the surface of the alloy. The difference between the mass growth of TiAl with and without Nb was 2 orders of magnitude.

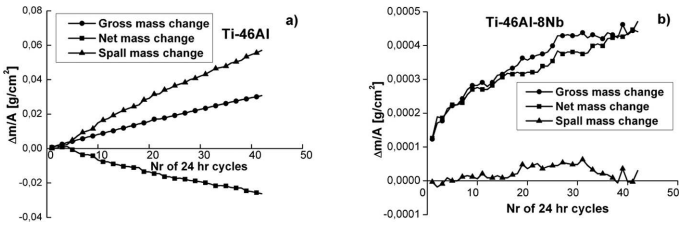

Fig. 5. Cyclic oxidation kinetics of a) Ti-46Al and b) Ti-46Al-8Nb at 1073 K in laboratory air for 42 cycles (1 cycle, 24 hrs)

X-ray Diffraction (XRD) patterns of Ti-46Al and Ti-46Al-8Nb after cyclic oxidation at 1073 K in laboratory air for 1008 hrs are illustrated in Fig. 6a and Fig. 6b, respectively. The XRD pattern of Ti-46Al is dominated by peaks of rutile and corundum. In addition, there are peaks of TiN, Ti_2AlN ternary nitride and Ti-Al phases from the metallic substrate. Similar phases were detected in the case of Ti-46Al-8Nb. Contrary to the isothermal XRD analysis, the presence of NbO was not detected. Due to the absence of separate Nb oxides, it can be supposed that this element substitutes titanium in the rutile lattice [15]. No Nb-containing phases were detected, probably indicating that Nb remains dissolved in titania, in nitrate and in the base intermetallic phase.

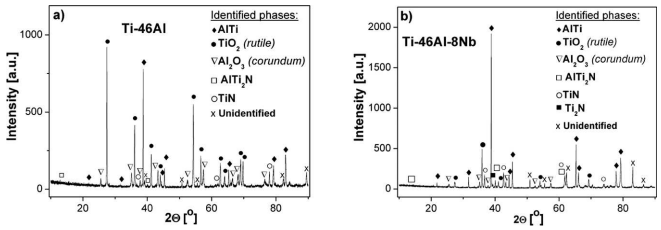

Fig. 6. X-ray Diffraction (XRD) analysis obtained on the surface of a) Ti-48Al and b) Ti-46Al-8Nb after cyclic oxidation at 1073 K in laboratory air for 1008 hrs

Cross-section morphologies of Ti-46Al and Ti-46Al-8Nb after cyclic oxidation in laboratory air for 1008 hrs. are presented in Fig. 7a and Fig. 7b, respectively. From Fig. 7a it follows that an oxide scale of around 50 μm thickness was formed on the Ti-46Al substrate. The afore-mentioned scale consists of a thin TiO_2 outer layer, below which Al_2O_3 and TiO_2 layers are stacked alternately on top of one another. Furthermore, the adherence between the scale and substrate is poor and cracks are visible in the scale. From Fig. 7b it follows that a much thinner scale (about 2-3 μm) is formed on Ti-46Al-8Nb. This layer, in turn, consists of an outer layer built of Al_2O_3 with the presence of some amounts of TiO_2 nodules, an intermediate layer of the scale consisting of a TiO_2, an inner layer of nitrides and niobium rich particles at the scale/substate interface. Moreover, the oxide scale is well adherent to the metallic substrate.

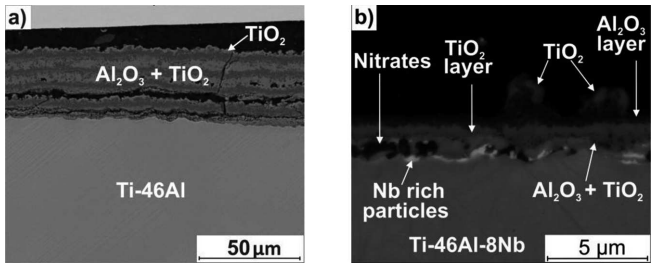

Fig. 7. SEM microphotograph of the oxide scale cross-section formed on a) Ti-48Al and b) Ti-46Al-8Nb after cyclic oxidation at 1073 K in laboratory air for 1008 hrs

4. Conclusions

The addition of 8 at.% niobium to γ-TiAl alloy significantly increases its resistance against both isothermal and cyclic oxidation in air and improves the adherence of the oxide scale formed during the corrosion process to the metallic substrate. It can also be concluded that the rate of oxide scale formation on γ-TiAl based intermetallics is dependent on a mixed diffusion process, consisting of outward titanium and niobium transport and predominant oxygen inward transport, both via lattice diffusion and through grain boundaries. The positive effect of niobium on the oxidation resistance of the alloy can be explained as the Nb ions in TiO_2 causing oxide vacancy concentration to decrease, thereby limiting the inward diffusion of oxygen. In addition, the niobium rich particles, formed during oxidation on the alloy/scale boundary, assume the role of a diffusion barrier.

Acknowledgements

This work has been supported by the Ministry of Science and Higher Education, Contract No: 330/N-POLONIUM/2008/0. The author is also grateful to Dr L. Niewolak from Forschungszentrum Julich, Germany for SNMS analysis, Dr J. Quaddakers for the discussion of SNMS profile and Prof. S. Chevalier for his assistance with the isotope studies.

REFERENCES

[1] G. Sauthoff, Mater. Corr. **47**, 589 (1996).
[2] S. Taniguchi, Developments in high-temperature corrosion and protection of materials, Cambridge, England 2008.
[3] E.A. Loria, Intermetallics **8**, 1339 (2000).
[4] S. Becker, A. Rahmel, M. Schorr, M. Schütze, Oxid. Met. **38**, 425 (1992).
[5] Y. Shida, H. Anada, Corr. Sci. **35**, 945 (1993).
[6] S.A. Kekare, P.B. Aswath, J. Mater. Sci. **32**, 2485 (1997).
[7] A. Gil, Wysokotemperaturowa korozja stopów TiAl, Krakow 2009.
[8] M. Yoshihara, K. Miura, Intermetallics **3**, 357 (1995).
[9] J.P. Lin, L.L. Zhao, G.Y. Li, L.Q. Zhang, X.P. Song, F. Ye, G.L. Chen, Intermetallics. **19**, 131 (2011).
[10] E. Godlewska, M. Mitoraj, J. Morgiel, Mater. High Temp. **26**, 99 (2009).
[11] V. Shemet, A.K. Tyagi, J.S. Becker, P. Lersch, L. Singheiser, W.J. Quadakkers, Oxid. Met. **54**, 211 (2000).
[12] M. Groβ, V. Kolarik, A. Rahmel, Oxid. Met. **48**, 171 (1997).
[13] G. Schumacher, F. Dettenwanger, M. Schütze, U. Hornauer, E. Richter, E. Wieser, W. Molier, Intermetallics **7**, 1113 (1999).
[14] J. Prażuch, K. Przybylski, S. Chevalier, T. Brylewski, Mater. Sci. Forum. **696**, 389 (2011).
[15] M. Pfeiler, C. Scheu, H. Hutter, J. Schnoller, J. Michotte, C. Mitterer, M. Kathrein, J. Vac. Sci. Technol. **A27**, 554 (2009).

Received: 20 January 2013.